Proteolytic Cleavage Sites of Native AE2 Anion Exchanger in Gastric Mucosal Membranes†

Alexander S. Zolotarev,‡ Marina N. Chernova,‡ Drakoulis Yannoukakos,‡,§ and Seth L. Alper*,‡,||,⊥

Molecular Medicine and Renal Units, Beth Israel Hospital, and Departments of Cell Biology and Medicine, Harvard Medical School, Boston, Massachusetts 02215

Received November 2, 1995; Revised Manuscript Received May 22, 1996⊗

ABSTRACT: The AE2 anion exchanger in pig and rabbit gastric mucosal membranes was subjected to limited proteolysis with trypsin, chymotrypsin, and papain, and to enzymatic N-deglycosylation. A monoclonal antibody to the AE2 C-terminal peptide was raised, characterized, and used to purify pig AE2 and its C-terminal cleavage products. Five distinct proteolytic cleavage sites within the AE2 transmembrane domain were defined by amino acid sequencing. The amino acid sequence of pig AE2 in the region encompassing the N-glycosylated Z-loop was also determined by RT-PCR. Tryptic cleavage of pig AE2 in the Z-loop produced C-terminal glycopeptides and was unaffected by deglycosylation, whereas the smaller rabbit AE2 C-terminal tryptic peptide lacked oligosaccharide, consistent with the respective amino acid sequences. The third consensus N-glycosylation site in pig Z-loop was heterogeneously glycosylated. Rapid papain cleavage in the Z-loop and slower cleavage in loop 7−8 produced C-terminal peptide products which were not N-glycosylated. Chymotryptic cleavage of the rabbit AE2 Z-loop required prior deglycosylation. Chymotryptic cleavage in the pig AE2 Z-loop produced C-terminal glycopeptides. Prior deglycosylation of pig AE2 unmasked novel, ionic strength-sensitive chymotryptic cleavage sites in the adjacent exofacial loop 7−8. These results provide experimental confirmation for some aspects of AE2 topography previously predicted from primary structure alone.

Limited enzymatic degradation is an important tool in the initial delimiting of folded domains of polypeptides. This process is especially important in the characterization of polytopic membrane glycoproteins. Transmembrane solute translocators comprise a major proportion of this class of proteins. One of the best studied of these is the erythroid anion exchanger protein, AE1. AE1 has been extensively analyzed by proteolytic digestion [as summarized by Jennings (1992)] and by deglycosylation (Casey et al., 1992). The abundance and relative purity of AE1 in the erythrocyte membrane has permitted crystallization of the AE1 membrane domain in two-dimensional sheets, enabling three-dimensional image reconstructions from electron microscopic analysis to a resolution of 20 Å (Wang et al., 1994). However, even the simpler biochemical analyses have not yet been extensively applied to the nonerythroid anion exchanger polypeptides in their native membranes.

The functional expression of heterologous AE2 in mammalian cells (Jiang & Alper, 1993; Lee et al., 1991), Sf9 insect cells (He et al., 1993), and *Xenopus* oocytes (Humphreys et al., 1994) and of AE3 in mammalian cells (Lee et al., 1991) and *Xenopus* oocytes (Yannoukakos et al., 1994) has opened the possibility for assignment of particular functional properties to delimited structural domains or even single amino acid residues of the AE2 and AE3 polypeptides. However, though AE2 and AE3 structures are modeled by analogy with AE1, biochemical data on the structures of AE2 and AE3 are meager.

Therefore, we have underaken studies of the limited proteolysis of native AE2 in basolateral membranes from pig and rabbit gastric mucosa, using immunoblot with antibodies raised against mouse AE2 C-terminal aa 1224−1237. We have defined C-terminal products of limited proteolytic digestion of AE2 and characterized their dependence on N-glycosylation state. In order to define the AE2 cleavage sites, we developed a monoclonal antibody to AE2, used it to purify AE2 C-terminal degradation products to homogeneity, and determined N-terminal amino acid sequences of those fragments.

Portions of this work were presented in preliminary form at annual meetings of the American Gastroenterological Association (Zolotarev & Alper, 1993b) and the American Society of Nephrology (Zolotarev & Alper, 1993a).

MATERIALS AND METHODS

Immunization and Hybridoma Production. A synthetic peptide containing the 14 C-terminal amino acid residues of mouse AE2 (MIT Biopolymers Laboratory) was coupled to keyhole limpet hemacyanin (KLH)[1] using succinimidyl 4-(*N*-maleimidomethyl)cyclohexane-1-carboxylate (SMCC, Pierce) as described (Alper et al., 1989). Peptide−KLH conjugate was stored in aliquots at −20 °C until use. Three Balb/c mice were each injected intraperitoneally with 100 μg of peptide−KLH conjugate in Freund's complete adjuvant.

† Supported by NIH DK43495 and a Pilot/Feasibility Award and the Molecular Biology Core Facility of the Harvard Digestive Diseases Center (DK34854).

* To whom correspondence should be addressed at Molecular Medicine Unit, Beth Israel Hospital RW763, 330 Brookline Ave., Boston, MA 02215. Tel: (617) 667-2930. FAX: (617) 667-2913. E-mail: salper@bih.harvard.edu.

‡ Molecular Medicine Unit, Beth Israel Hospital.

§ Current address: Demokritos National Center for Scientific Research, (153) 10 Ag. Paraskevi Attikis, P.O.B. 60228, Athens, Greece.

|| Renal Unit, Beth Israel Hospital.

⊥ Harvard Medical School.

⊗ Abstract published in *Advance ACS Abstracts,* July 15, 1996.

S0006-2960(95)02608-0 CCC: $12.00

Subsequent intraperitoneal injections in incomplete Freund's were administered at months 1, 1.5, 2, and 3. Four days before fusion, a final i.v. boost of peptide without adjuvant was administered. The mice were tail-bled, and resultant serum was screened by ELISA (see below) for the presence of antibodies against peptide−KLH conjugate. Cells from one half-spleen of the animal with the strongest immune response were fused with P3X63-AG8.653 myeloma cells (ATCC) as described (Kohler & Milstein, 1976). The cells were cultured in 96-well plates in RPMI 1640 medium containing 20% fetal calf serum, 10^{-4} M hypoxanthine, 4×10^{-7} M aminopterin, and 1.6×10^{-5} M thymidine (HAT medium).

Screening, Subcloning, and Antibody Production. After 10 days, the hybridoma culture fluids (50 μL) from 480 wells were screened by ELISA for the presence of antibody against peptide antigen coupled to BSA via *m*-maleimidobenzoyl-*N*-hydroxysuccinimide ester (MBS, Pierce). The assay used 0.2 μg of peptide−BSA conjugate adsorbed per well of PRO-BIND Assay Plate (Falcon). Following five washes with deionized water, the wells were blocked with 0.05% Tween 20/0.25% BSA/1 mM EDTA in borate-buffered saline (0.17 M H_3BO_4, 0.12 M NaCl, adjusted to pH 8.5 with NaOH) and incubated with culture fluid for 2 h. After washing as above, the wells were incubated for 1 h with 50 μL of alkaline phosphatase-conjugated affinity-purified goat anti-mouse IgG (H+L) (Jackson ImmunoResearch) diluted 1:1000 in blocking buffer. After subsequent washing, wells were developed with 1 mg/mL *p*-nitrophenyl phosphate (Sigma) in 10 mM diethanolamine, pH 9.5, 0.5 mM $MgCl_2$. Nonimmune mouse sera served as negative controls. Cells from positive wells were twice subcloned by limited dilution and rescreened. Determination of monoclonal antibody isotype was with the dipstick kit from Gibco BRL.

For production of antibody in higher quantity, Balb/c mice were primed with pristane (Harlow & Lane, 1988), followed by intraperitoneal injection with hybridoma cells ($\sim 10^6$ cells per mouse). Ascitic fluid drained from each mouse was incubated 1 h at 37 °C, then overnight at 4 °C. The hybridoma cells were separated by centrifugation for 10 min at 3000*g*, and aliquoted supernatants were frozen at −20 °C.

Limited Proteolysis of Stomach Membranes. 32/42 membranes isolated as previously described (Zolotarev et al., in press) were incubated with trypsin, chymotrypsin, or papain (Sigma) at the indicated w:w ratios, temperatures, and times. Proteolysis could not be quenched with addition of inhibitors, since the proteases remained active in the sodium dodecyl sulfate−polyacrylamide gel electrophoresis (SDS−PAGE) stacking gel; nor could the proteases be inactivated by boiling in SDS, since boiling rapidly promoted SDS-resistant aggregation of AE2 and of its C-terminal cleavage products. Therefore, protease reactions were terminated by addition of trichloracetic acid (TCA) to a final concentration of 7% at the indicated times (Arnon, 1970; Sweadner, 1991). Zero-time points in digestion experiments represented addition of TCA immediately following addition of protease. Quenched samples were pelleted by microfuge, washed in water to remove residual TCA, solubilized in SDS load buffer, and incubated at room temperature for 10−60 min prior to analysis on 5%−20% linear gradient SDS polyacrylamide minislab 0.75 mm gels by the method of Laemmli (1970).

After semidry transfer to BA-S 83 nitrocellulose (Schleicher & Schuell), AE2 proteolytic fragments were visualized on the nitrocellulose blots either with affinity-purified polyclonal rabbit antibody to mouse AE2 C-terminal aa 1224−1237 (Stuart-Tilley et al., 1994) or with mouse monoclonal antibody to the same antigen. Calculation of cleavage recoveries was not attempted, since polypeptide transfer efficiency varied as a function of peptide M_r.

In some experiments AE2 was deglycosylated with recombinant peptide:*N*-glycosidase F (PNGase F, New England Biolabs) before or after proteolysis. The usual deglycosylation buffer was 50 mM Tris, pH 7.6. When deglycosylation followed proteolysis, the reaction included 100 μg of PMSF/mL and 20 μg/mL each of chymostatin, pepstatin, aprotinin, antipain, and leupeptin (protease inhibitor cocktail). Pig 32/42 membranes were treated with 2500 units of PNGase F/mg of membrane protein.[2] Rabbit 32/42 membranes were treated with 1700 units of PNGase F/mg of membrane protein.

Immunoaffinity Isolation of AE2 C-Terminal Proteolytic Fragments. To obtain the AE2 fragment P35 in quantity sufficient for N-terminal amino acid sequencing, 25/42 membranes (50 mg of total protein in 15 mL) were treated with papain (20:1, w/w) for 1 h at 37 °C in 50 mM Tris-HCl, pH 7.6, 150 mM NaCl. Proteolysis was terminated by addition of iodoacetamide and sodium bicarbonate, pH 9.2, to respective final concentrations of 5 and 150 mM. Treated membranes were sedimented in a Sorvall T-865 rotor at 55 000 rpm for 25 min, resuspended, and resedimented twice more in 25 mL of the same buffer, and then solubilized at 4 °C for 30 min in 25 mL of 20 mM Tris-HCl, pH 7.6, 1% Triton X-100, 1 mM PMSF (solubilization buffer).

Insoluble material was removed by centrifugation, and to the Triton extract were added NaCl to 150 mM and 25 μL of crude ascites. After overnight incubation, 150 μL of protein G-agarose (50% vol/vol, Boehringer Mannheim) was added and incubation continued for an additional 2 h. Beads were batch-washed three times in 45 mL of wash buffer (20 mM Tris-HCl, pH 7.6, 150 mM NaCl, 0.2% Triton X-100), and then twice in 2 mL of elution buffer (20 mM Tris-HCl, pH 7.6, 1% CHAPSO, 1 mM DTT). P35 fragment was batch-eluted from the protein G-agarose beads for 1 h at 4 °C in 1 mL of elution buffer containing 0.5 mg of synthetic peptide antigen/mL. After removal of eluate, the beads were washed once more with the same solution, and pooled eluates were concentrated with a Centricon 10 concentrator. Detergent was removed from the sample by methanol/chloroform precipitation (Ran & Benos, 1992). To optimize

[1] Abbreviations: SMCC, succinimidyl 4-(*N*-maleimidomethyl)cyclohexane-1-carboxylate; MBS, *m*-maleimidobenzoyl-*N*-hydroxysuccinimide ester; PMSF, phenylmethylsulfonyl fluoride; PBS, phosphate-buffered saline; DIDS, 4,4′-diisothiocyanatostilbene-2,2′-disulfonic acid; PNGase F, peptide:*N*-glycosidase F; PAGE, polyacrylamide gel electrophoresis; TCA, trichloroacetic acid; TFA, trifluoroacetic acid; KLH, keyhole limpet hemocyanin; BSA, bovine serum albumin; T55, T40, T36, the AE2 C-terminal tryptic fragments of 55, 40, and 36 kDa, respectively; CH55, CH39, CH28/29, the AE2 C-terminal chymotryptic fragments of 55, 39, and 28/29 kDa, respectively; P35, P28/29, P22, the AE2 C-terminal papain fragments of 35, 28/29, and 22 kDa, respectively; 38K, the AE2 C-terminal fragment of 38 kDa generated by endogenous gastric membrane proteases concomitant with deglycosylation by PNGase F.

[2] One unit of PNGase F is defined as the amount of enzyme required to remove all of the carbohydrate from 10 μg of denatured RNase B at 37 °C in 1 h (500 New England Biolab units = 1 IUB milliunit).

yield and detection, the hydrophobic proteolytic fragments were disaggregated before SDS−PAGE by treatment with neat trifluoroacetic acid (TFA) (Hennessey & Scarborough, 1989).

The sample was electrophoresed (Laemmli, 1970) through 12% homogeneous polyacrylamide minigels (10 × 8 cm, 1.5 mm thick, 10-well comb) at constant amperage (40 mA). The P35 fragment was transferred to PVDF membrane (Immobilon-P^{SQ}, Millipore) at 2 mA/cm^2 for 1 h in a blotting buffer of 10 mM CAPS, pH 11, in 10% MeOH, 0.2% SDS (LeGendre & Matsudaira, 1989), using a semidry electroblotter (Panther, Owl Scientific). The Coomassie Blue R250-stained sample on PVDF was analyzed by Edman degradation on an Applied Biosystems gas phase sequenator (MIT Biopolymers Laboratory, Cambridge, MA).

Isolation and sequencing of the P28 fragment of AE2 was by the same methods, except that papain digestion of the 25/42 membranes was carried out in 20 mM HEPES/Tris, pH 7.6, rather than at physiological ionic strength.

For preparation of T40 for amino acid sequencing, 25/42 membranes (180 mg of protein in 30 mL) were incubated with trypsin (1:200, w/w) for 1 h at 37 °C in 150 mM NaCl, 50 mM HEPES/Tris, pH 7.4. Tryptic digestion was terminated by addition of PMSF to a final concentration of 1 mM. All further steps were in the presence of 1 mM PMSF. Membranes were washed in the same buffer and solubilized in 1% Triton X-100. The C-terminal AE2 glycopeptide T55 was affinity- purified as described above for P35 with proportionate scaleup, except that elution buffer contained 0.1% Triton X-100 instead of CHAPSO. T55 was eluted with peptide antigen and concentrated to 270 μL and then incubated overnight at 4 °C with 2000 units of PNGase F. T40 was prepared by SDS−PAGE in an 8% acrylamide gel and blotted to PVDF membranes as described above.

To isolate the T20 AE2 fragment, 25/42 membranes (50 mg of total protein) were solubilized in 25 mL as above, adjusted to 150 mM NaCl, and incubated 4 h at 4 °C with 50 μL of ascites and then overnight with 400 μL of protein G-agarose. The beads were washed, treated for 1 h at 4 °C with 1 μg of trypsin/mL in wash buffer, and extensively washed first with wash buffer and then with elution buffer. The T20 AE2 fragment was then eluted from the affinity matrix overnight with 0.5 mg of synthetic peptide antigen/mL and prepared for sequencing as described for P35.

DNA Cloning and Sequencing. Oligonucleotides encoding nt 2606−2622 and 2949−2931 of the murine AE2 sequence (Alper et al., 1988) were prepared by solid-phase synthesis on a Millipore oligonucleotide synthesizer. These sequences are perfectly conserved among AE2 cDNAs from mouse, rat, rabbit, and human. Total RNA was prepared from fresh pig fundic mucosa by the method of (Chirgwin et al., 1979). Reverse transcription-polymerase chain reaction (RT-PCR) was performed (Kawasaki, 1990) in a Perkin-Elmer 4800 DNA thermal cycler with 35 cycles of 1 min denaturation at 95 °C, 2 min annealing at 55 °C, and 3 min extension at 72 °C. The 100 μL reaction mixture contained template, 20 pmol of each primer, 500 μM dNTPs, 2−5 units of Taq DNA polymerase (Promega), and the manufacturer's buffer system. Reaction products were isolated on agarose gels, excised, purified, and directly sequenced on both strands by Taq cycle sequencing on an ABI automated DNA sequencer.

RESULTS

Production and Characterization of Monoclonal Antibodies. Attempts to elicit murine monoclonal antibodies against pig AE2 holoprotein purified in SDS (Zolotarev et al., in press) were unsuccessful. One of three mice immunized with mouse AE2 peptide 1224−1237 conjugated to KLH developed a high-titer immune response as judged by peptide ELISA and by AE2 immunoblot. From this mouse, only one ELISA-positive hybridoma (ZC-5−5) reacted equally with KLH−SMCC−peptide conjugate, BSA−MBS−peptide conjugate, and pure synthetic peptide and also detected AE2 by immunoblot of 32/42 membranes isolated from pig and from rabbit gastric mucosa. Later experiments further demonstrated immunoblot reactivity with gastric AE2 from mouse, rat, and human and competence as an immunoprecipitation reagent. The ZC-5−5 hybridoma produced up to 10 mg of monoclonal IgG3/mL of ascitic fluid.

Proteolysis of AE2 in Membranes. Gastric mucosal 32/42 membranes were subjected to timed proteolytic digestion and analyzed by immunoblot to define protease-resistant domains of native plasmalemmal AE2. Tryptic digestion of pig membranes at 20 °C produced within 10 min a set of stable C-terminal AE2 fragments centered at 55 kDa (Figure 1A, T55). Subsequent treatment with PNGase F reduced this group of fragments to a relatively uniform 40 kDa band (T40), documenting the 55 kDa complex as *N*-glycopeptides. When membranes were first deglycosylated and subsequently trypsinized, T40 again was the product (Figure 1B). The very sharp 38 kDa band (Figure 1B) which migrated below T40 was a product of endogenous protease activity which appeared only following deglycosylation of pig AE2 (Zolotarev et al., in press).

Trypsinization of rabbit membranes rapidly produced a stable, C-terminal band of 36 kDa (T36, Figure 1C). T36 did not change in mobility upon subsequent treatment with PNGase F, indicating that it did not bear N-linked oligosaccharide. Putative SDS-resistant dimers of AE2 C-terminal tryptic fragments also accumulated in both pig and rabbit membranes (*T55d, T40d, T36d*). Peptide competition abolished immunoblot detection of both monomeric AE2 bands and those which migrated as dimers (not shown). The time course of appearance and disappearance of the putative dimer bands always paralleled or followed that of the monomeric fragments (see, for example, Figures 1C and 2). Conditions that altered generation of monomeric fragments generally altered generation of the putative dimers as well (see, for example, Figure 4). The extent of this putative fragment dimerization varied among membrane preparations and experiments. Stable SDS-resistant dimers of hydrophobic fragments of the human AE1 transmembrane domain have been noted previously (Jennings et al., 1984).

Papain digestion of 32/42 membranes from both pig and rabbit rapidly yielded 35 kDa C-terminal peptides (Figure 2, P35). In pig membranes, further digestion yielded a pair of peptides of 29 and 28 kDa (P28/29) which were stable for 6 h, and a 22 kDa fragment (P22) which was evident after 22 h. Longer monitoring of pig AE2 digestion by papain was prevented by time-dependent aggregation of the cleavage products. The P35 fragment of rabbit was more stable than that of pig, but prolonged papain digestion produced fragments of 29, 28, and 22 kDa which comigrated with those from pig.

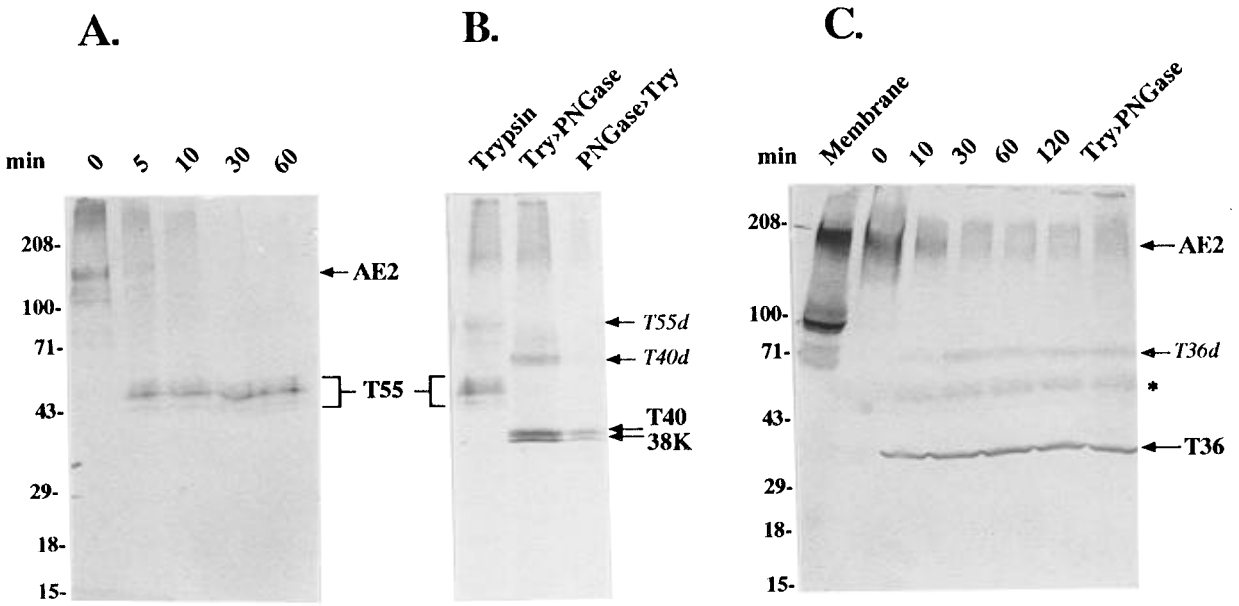

FIGURE 1: C-terminal AE2 immunoblot of pig and rabbit 32/42 gastric membranes following tryptic digestion in 50 mM Tris, pH 7.6. (A) Pig membranes were digested at 20 °C for the indicated times with trypsin 1:200 (w/w). (B) Effect of deglycosylation on trypsin digestion of pig AE2. Left lane: Following 30 min tryptic digestion at 20 °C, membranes were incubated at 37 °C for an additional 60 min in the presence of protease inhibitors. Middle lane: Membranes were treated with trypsin for 30 min at 20 °C, followed by PNGase F in 50 mM Tris, pH 7.6, for 60 min at 37 °C. Right lane: Membranes were incubated 60 min at 37 °C with PNGase F, followed by 30 min of tryptic digestion at 20 °C. (C) Rabbit membranes were digested at 37 °C for the indicated times with trypsin 1:50 (w:w). In the rightmost lane, membranes previously digested with trypsin for 60 min were further incubated in the presence of protease inhibitors with PNGase F for 60 min at 37 °C. Tryptic products of AE2 are denoted T55, etc. Putative dimers of these products are denoted by *T55d*, etc. The asterisk marks nonspecific bands in rabbit membranes which are labeled by nonimmune serum and not labeled by monoclonal anti-AE2 (not shown).

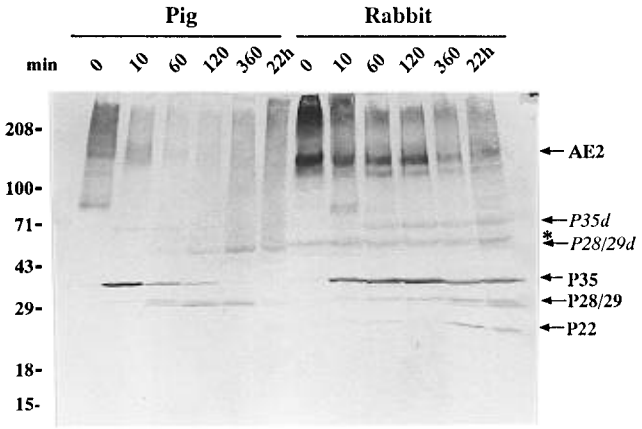

FIGURE 2: C-terminal AE2 immunoblot following papain digestion (1:20, w/w) of 32/42 gastric membranes of pig and rabbit at 37 °C in 50 mM Tris-HCl, pH 7.6, for the indicated times. Papain digestion products of AE2 are denoted with P; putative dimers are denoted by italics; the asterisk marks a nonspecific band in rabbit membranes.

Chymotrypsin digestion of 32/42 membranes from pig yielded a cluster of C-terminal fragments centered around 55 kDa (Figure 3A, CH55) which comigrated with the T55 peptides of AE2 (Figure 1A; see also below, Figure 4A, lanes 4 and 8). Subsequent deglycosylation reduced the CH55 complex to a single band of 39 kDa (CH39), whose leading edge comigrated with and sometimes obscured the 38 kDa endogenous cleavage product (Figure 3B). If, however, N-deglycosylation preceded chymotrypsin treatment, a stable C-terminal fragment of 29 kDa (CH29) was generated, consistent with unmasking of at least one new chymotryptic cleavage site at considerable distance in the linear sequence from the consensus glycosylation sites (Figure 3B). Sometimes a CH28/29 doublet was apparent (see below, Figure 4B), suggesting a second nearby cleavage site unmasked by N-deglycosylation. CH28/29 was never produced by chymotryptic digestion of native, glycosylated AE2 under any conditions tested.

Chymotryptic digestion of native rabbit AE2 did not produce immunospecific fragments containing intact C-terminal epitope (Figure 3C, left half). The 55 kDa bands (Figure 3C, asterisk) that appeared to increase slowly in intensity during chymotryptic digesion were considered nonspecific; these bands were detected with equal intensity by nonimmune serum but not detected by monoclonal antibody ZC-5−5 to the same AE2 C-terminal epitope (not shown). In addition, the time-dependent loss of total immunostaining intensity (Figure 3C, left half) suggested proteolytic loss of the AE2 C-terminal epitope mediated by chymotrypsin rather than generation of intact C-terminal fragments. In contrast, chymotrypsin treatment of deglycosylated rabbit membranes rapidly produced a metastable AE2 C-terminal fragment of 35 kDa (CH35). Digestion of deglycosylated AE2 for 30 min or longer yielded at low efficiency chymotryptic fragments of 29, 28, and 22 kDa (Figure 3C, right half).

Effects of Ionic Strength and Anions on Proteolytic Digestion of Pig AE2 in Membranes. To optimize preparative yield of proteolytic fragments for amino acid sequencing, and in view of the known sensitivity to ionic strength of proteolytic digestion of native erythroid AE1 (Jenkins & Tanner, 1977; Jennings et al., 1986; Makino et al., 1984), the effects of ionic strength were examined on digestion of pig gastric AE2 (Figure 4). Tryptic generation of both T55 from AE2 (Figure 4A, lanes 1−4) and of T40 from N-deglycosylated AE2 (Figure 4B, lanes 1−4) were relatively insensitive to the composition of the digestion buffer. The lowest yield of both fragments was observed in 50 mM Tris-HCl. CH55, the chymotryptic product of glycosylated

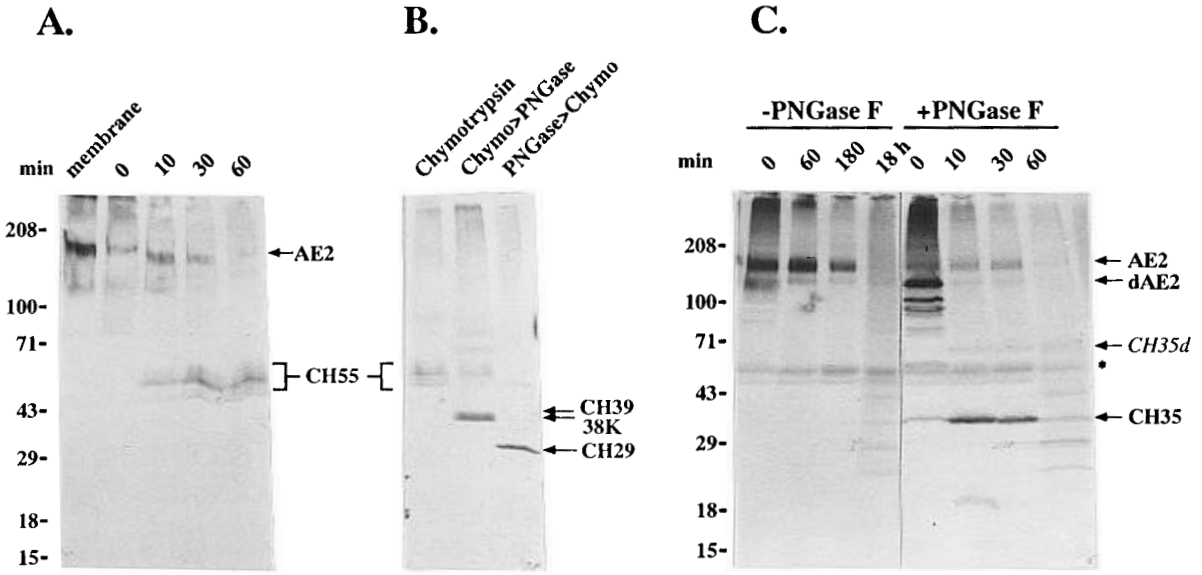

FIGURE 3: C-terminal AE2 immunoblot following chymotrypsin digestion (1:50, w/w) of 32/42 gastric membranes in 50 mM Tris, pH 7.6, at 37 °C. (A) Pig membranes were digested for the indicated times. (B) Left lane: pig membranes were treated with chymotrypsin for 60 min and then incubated in the presence of protease inhibitors for an additional 60 min at 37 °C. Middle lane: chymotrypsin-digested membranes were treated with PNGase F plus protease inhibitors for 60 min at 37 °C. Right lane: Membranes first treated with PNGase F for 60 min at 37 °C were then digested with chymotrypsin as above. (C) Rabbit membranes pretreated in the absence or presence of PNGase F for 60 min at 37 °C were digested with chymotrypsin for the indicated times. Chymotryptic products of AE2 are denoted with CH; the putative dimer is denoted by italics; the asterisk marks the same nonspecific band of rabbit membranes similarly noted in Figure 1C.

AE2, accumulated to higher levels in the presence of added 140 mM chloride or 140 mM nominal bicarbonate than in their absence (Figure 4A, lanes 5−8). In contrast, accumulation of CH28/29 from chymotryptic digestion of N-deglycosylated AE2 was greatest at low ionic strength (Figure 4B, lanes 5−8). Though CH28/29 rapidly accumulated to maximal levels in the presence of 20 mM HEPES/Tris and in isotonic sucrose, these cleavages were greatly inhibited in isotonic chloride or bicarbonate, such that some CH39 remained intact after 1 h of digestion at 37 °C.

Inhibition of AE2 proteolysis by 140 mM chloride and bicarbonate solutions was also evident in the generation by papain of P28/29, with corresponding accumulation of P35 (Figure 4A,B, lanes 9−12). However, the cleavage by papain which produced P28/29 was more potently inhibited by elevation of buffer concentration from 20 mM (Figure 4A,B, lane 9) to 50 mM (lane 11) than was the corresponding chymotryptic cleavage (Figure 4B, compare lanes 5 and 7). Figure 4 also shows that the rate of proteolytic loss of the AE2 C-terminal epitope itself varied according to ionic conditions, as judged by varying recoveries of immunoblot signal. This proteolytic loss of the epitope was not prevented by the presence of an estimated 10-fold molar excess of monoclonal antibody during digestion (not shown).

Partial cDNA Sequence of Pig AE2. The size of the T40 fragment derived from deglycosylation of pig AE2 T55 fragment (Figure 1B) suggested localization of the tryptic cleavage site within the 5−6 ecto-loop, on the N-terminal side of the loop's third consensus N-linked glycosylation site (Opdenakker et al., 1993). However, among the four published deduced amino acid sequences for AE2 there are no Lys or Arg residues in this region except for those homologous to the AE1 Lys residue(s) which comprise the covalent binding site for the isothiocyanate moieties of DIDS and other stilbene isothiocyanates (Wood, 1992). Moreover, treatment of pig 32/42 membranes with DIDS at concentrations up to 1 mM did not prevent subsequent generation of T40 by incubation with PNGase F followed by trypsin digestion (not shown). Therefore, we deduced the amino acid sequence of putative transmembrane spans 5 and 6 of pig AE2 and the connecting exofacial loop (Z-loop) from RT-PCR amplification and cDNA sequencing.

Figure 6A presents the amino acid sequence deduced from pig AE2 cDNA in alignment with other AE2 sequences extending from mouse aa 815 to 895. As predicted by the size of the pig AE2 C-terminal tryptic fragment, pig AE2 has an Arg at the position of mouse aa 869, rather than Trp or Gly as in other species. This Arg could account for the glycosylated T55 and deglycosylated T40 fragments of pig AE2. Mouse AE2 Ser 879, in the middle of the third consensus N-linked glycosylation site, is Arg in rabbit but Gly in pig. This Arg could account for the production of rabbit T36. In addition, pig AE2 has a three-residue insertion of Asp-Gly-Pro following mouse aa 881. These differences together might plausibly account for the size difference between pig T40 and rabbit T36. However, Raida et al. (1989) reported that the mouse AE1 C-terminal chymotryptic peptide was 6 kDa larger than the human peptide, despite being six amino acids shorter in length. Thus M_r and molecular weight for the transmembrane domains of AE anion exchangers do not strictly correspond.

Direct Sequencing of Pig AE2 C-Terminal Fragments. Current models of AE2 polypeptide folding in the membrane are based solely on hydropathy plots of deduced amino acid sequences and on analogy with vectorial labeling and proteolysis studies of red cell AE1. Immunoaffinity purification of the C-terminal fragments of native pig AE2 produced by papain digestion of gastric membranes allowed generation of peptide sequence. Edman degradation of the P35 fragment (initial yield, ~4.2 pmol) revealed unambiguous sequence through 11 cycles. P35 was produced by cleavage of AE2 within the "Z-loop" which connects the

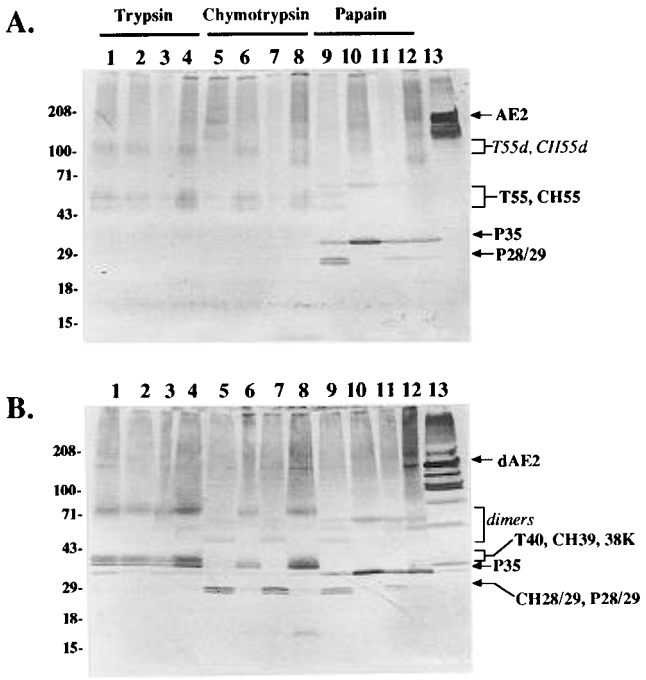

FIGURE 4: Effects of ionic strength, chloride, and bicarbonate on C-terminal proteolytic digestion of native AE2 (A) and of PNGase F-deglycosylated AE2 (B). Native or deglycosylated 32/42 pig membranes were digested with trypsin (1:200, lanes 1−4), chymotrypsin (1:50, lanes 5−8), or papain (1:20, lanes 9−12) for 60 min at 37 °C. Proteolysis buffer was 20 mM HEPES/Tris, pH 7.6 (lanes 1, 5, 9) or 50 mM Tris-HCl, pH 7.6, in the presence of 140 mM NaCl (lanes 2, 6, 10), 280 mM sucrose (lanes 3, 7, 11), or 140 mM sodium bicarbonate (lanes 4, 8, 12). Exogenous protease was omitted from the incubations in lane 13 of both panels. The AE2 in membranes of this figure was more degraded than those of Figure 3A (lane labeled "membrane"), as evidenced by the smear below AE2 (panel A, lane 13). These N-terminally truncated AE2 degradation products were well resolved following deglycosylation (panel B, lane 13).

exoplasmic ends of TM5 and TM6 (Figure 6A). The cleavable Gly-Arg bond lies five amino acid residues before the putative start of TM6 (Wood, 1992), is conserved between pig and rabbit AE2 sequences, and generates similar P35 fragments from pig and rabbit membranes (Figure 2). This glycine residue is glutamate in the mouse AE2 sequence, but Glu-X and Gly-X peptide bonds are hydrolyzed by papain at similar rates (Arnon, 1970). Thus, the P35 fragment produced upon cleavage of mouse AE2 in intact *Xenopus* oocytes (Zhang et al., in press) may originate from the same region of the Z-loop.

The lower yield of P28 fragment (∼2 pmol) allowed only five cycles of Edman degradation and yielded the N-terminal sequence of Ala-Pro-Glu-Lys-Arg. This sequence is identical to a stretch of the putative 7−8 ecto-loop of human AE2 and contains only one conservative substitution of Glu for Asp when compared with mouse, rat, and rabbit (Figure 6B).

Figure 5A shows AE2 C-terminal immunoblots of affinity-purified tryptic fragments of AE2 before (lane 1) and after deglycosylation (lane 2).

N-deglycosylation of T55 in the presence of Triton X-100 yielded T40, as was noted in intact membranes. The smaller AE2 C-terminal bands migrating below T40 were generated prior to the deglycosylation reaction (as judged from their presence in both lanes 1 and 2). Moreover, these smaller products were not produced when tryptic digestion was terminated by TCA (compare with Figure 4A, lanes 1−4).

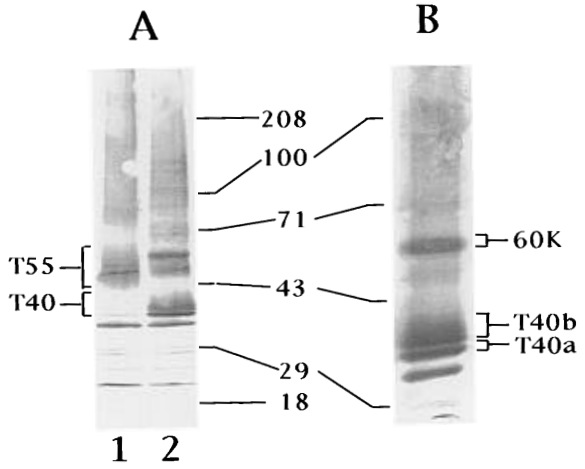

FIGURE 5: Immunoblot of purified AE2 C-terminal tryptic peptides. Triton X-100 lysates of trypsinized 32/42 gastric membranes were incubated with immobilized anti-AE2 mAb ZC-5−5. C-terminal AE2 tryptic fragments were eluted with peptide antigen. (A) 1% of the eluate was run on 5%−20% gradient SDS−PAGE and blotted to nitrocellulose (lane 1). Lane 2 shows 1% of the eluate remaining after PNGase F treatment. (B) The remaining N-deglycosylated sample was electrophoresed in two lanes on 8% SDS−PAGE and transferred to PVDF. 1% of this sample (shown) was used to immunolocalize the indicated AE2 C-terminal fragments. The corresponding regions of the adjacent lane were submitted for amino acid sequencing (Table 1).

For these reasons, we attribute these smaller AE2 fragments to residual tryptic activity in detergent-solubilized trypsinized membranes.

The affinity-purified T40 (Figure 5) was more clearly heterogeneous than had been apparent when deglycosylation was carried out in native membranes (see, for example, Figures 1B and 4B, lanes 1−4). To evaluate the source of this heterogeneity we sequenced separately the leading edge (T40a, 29 cycles of Edman degradation) and the trailing smear (T40b, 20 cycles) of T40. Figure 5B shows these two portions of T40 as submitted for sequencing from PVDF membrane.

T40a and T40b yielded identical N-terminal amino acid sequences (Table 1) which resulted from hydrolysis of the Arg55-Ala56 bond in the Z-loop of pig AE2 (Figure 6A). This sequence is identical with that deduced from the PCR-amplified cDNA (Figure 6A) with one exception. Asn64 in the deduced pig AE2 sequence is replaced in T40a and T40b by Asp (cycle 9), reflecting the amidase activity of PNGase F (Tarentino et al., 1990). The molar yields of Asp from Edman degradation of T40a and T40b were comparable to that of the surrounding Gly residues (Table 1), indicating that N-degylcosylation proceeded nearly to completion. In contrast, the molar yield of Thr at cycle four of T40b was only 12% of that of the preceeding Ala, whereas cycle four of T40a produced Thr at a yield of 44% of the preceding Ala, normal for this sequenator.

Edman degradation of the C-terminal AE2-immunoreactive band of M_r 60 kDa (60K in Figure 5B) revealed the presence of more than one sequence, with the predominant sequence of Ala-Leu-Leu-Gln-Met-Val. This sequence, conserved among all sequenced AE2s, corresponds to aa 655−660 of mouse AE2. The sequence is consistent with tryptic cleavage at the Lys654−Ala655 bond, located 48 residues prior to the putative start of TM1 (Wood et al., 1992). This site aligns closely with the chymotryptic and tryptic cleavage

Table 1: Edman Degradation of the T40 Fragments of Pig AE2

cycle no.	1	2	3	4	5	6	7	8	9	10	11	12	13	14	15	16	17	18	19	20	21	22	23	24	25	26	27	28	29
sequence	Ala	Ala	Ala	Thr	Thr	Gln	Pro	Gly	Asp	Gly	Ser	Ser	Ala	Gly	Pro	Ala	Gly	Pro	Ser	Gly	Gln	Gly	Arg	Pro	Arg	Gly	Gln	Pro	Asn
T40a[a]	41.3	37.4	37.5	16.4	20.0	28.1	29.3	24.6	23.0	20.8	7.6	5.6	16.4	13.3	11.0	11.6	9.8	6.6	2.9	7.6	4.2	4.8	3.8	1.6	1.8	2.1	1.6	0.6	1.1
T40b[a]	38.8	35.3	32.5	3.9	18.3	18.0	17.5	14.4	14.5	9.7	5.1	5.8	9.1	6.8	6.2	6.1	4.9	3.6	1.2	2.2									

[a] Yield of amino acid residues on each cycle of Edman degradation, shown in pmol.

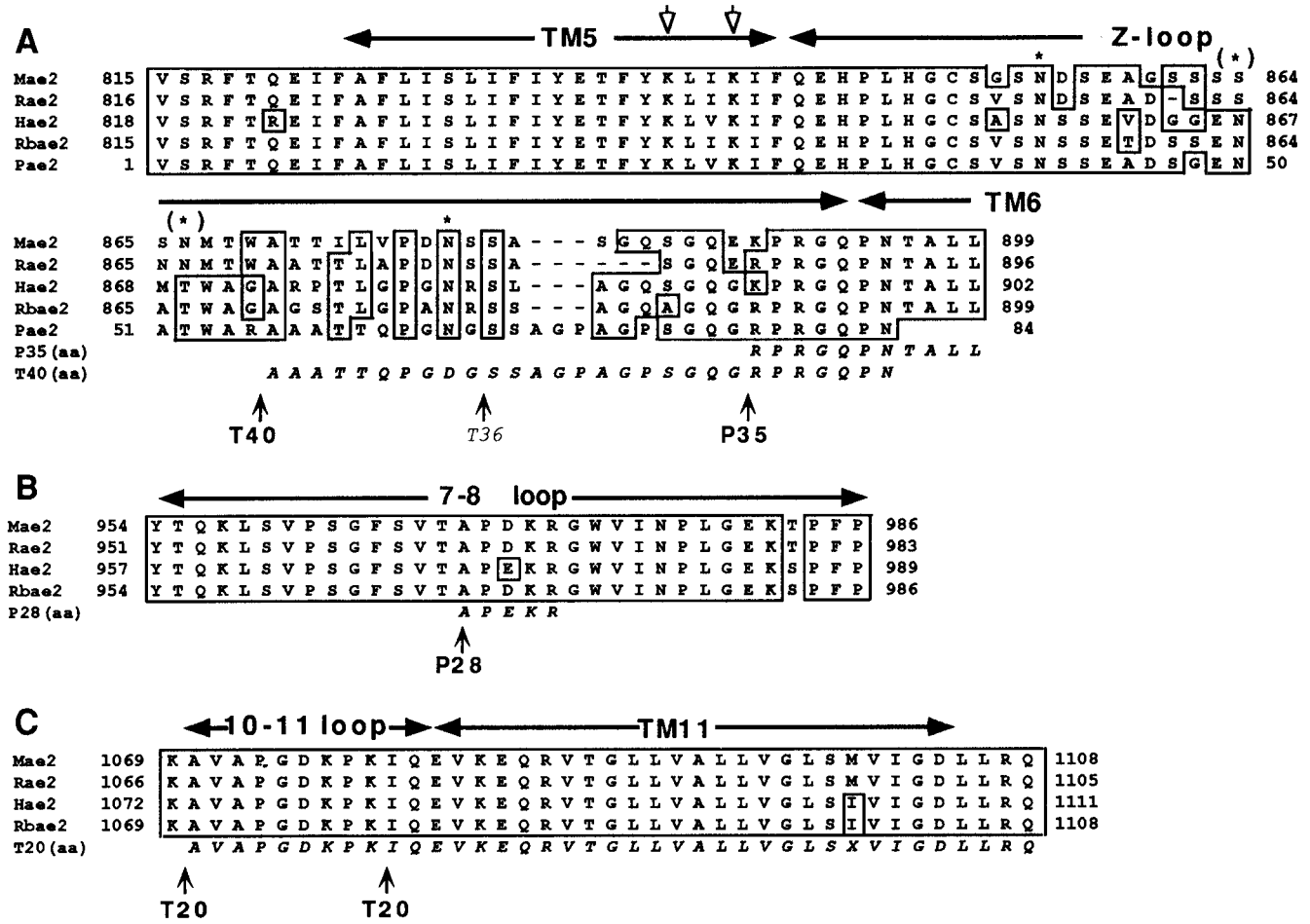

FIGURE 6: (A) Alignment with published mammalian AE2 amino acid sequences of the sequence of pig AE2 corresponding to TM5, TM6, and the extracellular Z-loop connecting them. Open arrowheads denote the conserved DIDS-binding lysines. Asterisks mark conserved N-linked glycosylation sites. Asterisks within parentheses mark non-conserved glycosylation sites. Amino acid (aa) sequences from Edman degradation are indicated in italic capitals. Arrows mark the sequenced T40 and P35 sites of pig AE2 and the postulated T36 site (italics) of rabbit AE2; Mae2, mouse AE2 (Alper et al., 1988); Rae2, rat AE2 (Lindsey et al., 1990); Hae2, human AE2 (Gehrig et al., 1992); Rbae2, rabbit AE2 (Chow et al., 1992); Pae2, pig AE2 amino acid sequence deduced from cDNA. (B) AE2 amino acid sequences corresponding to the putatively exofacial loop connecting TM7 and TM8. Arrow marks the sequenced P28 site. (C) AE2 amino acid sequences corresponding to the putative endofacial loop between TM10 and TM11 and to the adjacent putative TM11. Closed arrows mark the sequenced T20 sites.

sites at Tyr359 and Lys360 of human AE1 (Mawby & Findlay, 1982). Thus, the 60K band of AE2 in Figure 5B is the N-deglycosylated membrane domain of AE2 (Figure 7) and is analogous to the T52 tryptic fragment of human AE1 (Jennings et al., 1986).

To gain additional information about protein folding in the membrane, AE2 was solubilized in Triton X-100. Such treatment renders additional peptide bonds exposed on the protein surface accessible to proteolytic attack (Makino et al., 1984). To preserve the C-terminal epitope of AE2 required for subsequent purification of the proteolytic fragments, the proteolysis was carried out after AE2 was bound to the monoclonal antibody. The feasibility of this approach depends upon the relative rates of proteolysis of the protein under study and the antibody. Accumulation of a proteolytic fragment (T20) from the transmembrane domain of AE2 was observed only after addition of trypsin. In contrast, papain hydrolyzed bound antibody faster than AE2, and chymotrypsin hydrolyzed antibody and AE2 at equal rates (not shown).

From detergent extract of 50 mg of membrane protein was obtained ~200 pmol of T20 on PVDF membrane. Application of ~100 pmol to the sequenator revealed the presence of two sequences within the T20 band. The principal sequence, comprising 80% on a molar basis, extended 38 amino acid residues. The less abundant sequence (20% on a molar basis) was identical to the major sequence except for the absence of its nine N-terminal residues (Figure 6C). Thus, trypsin cleaved Triton X-100-solubilized AE2 at two sites within the putative endo-loop connecting TM10 and TM11. The more N-terminal site corresponds to the tryptic endo-site of AE1 reported by Jennings and colleagues (1986).

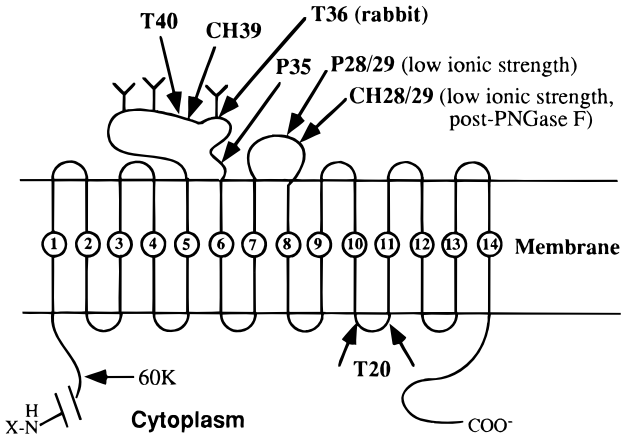

FIGURE 7: Schematic topographical profile of pig AE2 polypeptide, with approximate locations of N-linked glycosylation sites and proteolytic cleavage sites noted. Fragment abbreviations are as defined previously. N-terminus is blocked (X).

DISCUSSION

The results presented above comprise the first biochemical studies on native AE2 polypeptide. Proteolytic cleavage sites in the transmembrane domain of AE2 were defined for trypsin, chymotrypsin, and papain. The removal of N-linked oligosaccharides by PNGase F led to exposure of chymotryptic cleavage sites which displayed sensitivity to ionic strength. Three cleavage sites were defined in native pig AE2 by N-terminal amino acid sequencing of purified C-terminal fragments T40, P35, and P28. Two additional cleavage sites was defined in Triton-solubilized pig AE2 by N-terminal sequencing of purified T20 fragment. The amino acid sequence of the pig AE2 Z-loop deduced from the corresponding cDNA sequence, together with the N-terminal amino acid sequence of the T40 fragment, provided an explanation for the different sizes of tryptic fragments generated from pig and rabbit AE2. The schematic drawing in Figure 7 summarizes the proteolytic cleavage data for pig AE2.

Current topographical models of AE2 (Wood, 1992) based on hydropathy calculations and on comparison with AE1 suggest the presence of two large exofacial loops, the 5−6 loop (Z-loop) and the 7−8 loop, which by virtue of size are likely sites for external proteolytic cleavage. Hypothetical C-terminal AE2 peptides starting at either end of the Z-loop have predicted molecular masses of 43.5 and 38 kDa. C-terminal AE2 peptides beginning at either end of the 7−8 ecto-loop have predicted molecular masses of 31.5 and 28 kDa. The P35 fragment of AE2 is ~3 kDa smaller than the smallest predicted Z-loop fragment and might better correspond in size to a cleavage site in the 6−7 endo-loop. However, comparison of the N-terminal amino acid sequence of the pig P35 fragment with the pig Z-loop cDNA sequence situates this papain cleavage site within the Z-loop, five amino acid residues N-terminal to the putative start of TM6 (Figure 6A). The P35 fragments from AE2 of pig and of rabbit displayed identical electrophoretic mobility (Figure 2). In addition, the amino acid sequences of pig and rabbit AE2 are identical in the region of the P35 cleavage site (Figure 6A). Together, these observations allow the prediction that papain cleaves rabbit AE2 in intact gastric membranes at its Gly888-Arg889 bond.

This predicted exofacial position of the P35 cleavage site (Figure 7) is consistent with the generation by extracellular papain digestion of a P35-like C-terminal AE2 fragment from mouse AE2 expressed in *Xenopus* oocytes (Zhang et al., 1996). A similar exofacial papain cleavage site in native human erythroid AE1 was localized three amino acid residues N-terminal to the putative start of TM6 (Jennings et al., 1984). In addition, the pig P35 cleavage site aligns well with the exofacial chymotryptic cleavage site at Lys 578 in native mouse erythroid AE1 (Raida et al., 1989).

The 6 kDa difference between P35 and the P28/29 fragments suggest the assignment of the P28/29 sites to the 7−8 ecto-loop (Figure 7). Direct protein sequencing of the pig P28 peptide was consistent with this localization (Figure 6B). Interestingly, the N-terminal Ala of the P28/29 fragment corresponds in the aligned sequences of mammalian AE1 proteins to the glycosylated Asn of the exofacial 7−8 loop.

The schematic in Figure 7 places the pig AE2 cleavage sites which generate T40 and CH39 between the second and third N-linked glycosylation sites of the Z-loop. The rabbit T36 site is placed after the third Z-loop glycosylation site. The only Arg in the rabbit Z-loop, Arg879, resides immediately C-terminal to the third consensus N-glycosylation site, Asn878. The nine amino acid residues (Figure 6A) which separate Arg879 and Gly888 (the site of papain attack predicted above) fit the observed difference in electrophoretic mobility between rabbit fragments T36 and P35. Such placement of the rabbit tryptic cleavage site is also consistent with the observation that T36 migrated as a sharp band (Figure 1C) which did not change mobility upon PNGase F treatment.

The ~5 kDa difference in electrophoretic mobility between pig T40 and P35 fragments suggests a possible tryptic cleavage site within the stilbene isothiocyanate binding site KLVK (residues 24−27, Figure 6A) located at the ecto-terminus of TM5 (Figure 7). However, two indirect results argue against this possibility. First, prolonged treatment of unsealed pig gastric membranes with 1 mM DIDS prior to deglycosylation and trypsin treatment did not inhibit generation of T40 (not shown). Second, the KLI/VK sequence is conserved in AE1, in which it is resistant to tryptic cleavage in the absence or presence of DIDS (Landolt-Marticorena et al., 1995; Okubo et al., 1994). Finally, the N-terminal amino acid sequence of the T40 fragment directly proves that trypsin cleaves pig AE2 in the middle of the Z-loop at Arg55 (Figure 6A).

The difference in size between the AE2 C-terminal tryptic and papain fragments is 22 amino acids, predicting a difference in electrophoretic mobility of only ~2.4 kDa. This contrasts with the observed size difference of 5 kDa between T40 and P35. The discrepancy may result only from altered SDS-binding to the polypeptides. However, the N-deglycosylated T40 band (Figure 4B, lane 4) is wider and more diffuse than the bands of P35 (lane 10) or CH28/29 (lane 5), a characteristic shared with CH39 (lane 8). Moreover, electrophoresis of the affinity-purified T40 fragment revealed its heterogeneity (Figure 5). The absence of asparagine in T40a and T40b at cycle 9 of Edman degradation (Table 1), together with the PNGase F-induced mobility shift from T55 to T40, excludes incomplete N-deglycosylation as a cause of the heterogeneity. Thus, the Z-loop of pig AE2 likely bears another type of posttranslational modification between Arg55 and Arg78. The presence of GalNAc in the monosaccharide analysis of AE2 (Zolotarev et al., 1996), as well as

the presence of several Thr and Ser residues between the T40 and P35 sites of pig AE2 (Figure 6A), suggests the presence of O-glycosides in this region of the protein. The extremely low yield of Thr from Edman cycle 4 of T40b is also consistent with O-glycosylation of this amino acid residue, but direct evidence for *O*-glycoside in AE2 of any species remains lacking.

Limited proteolysis of pig AE2 in native membranes produced no detectable T20 fragment under any tested condition. Incubation of membranes with trypsin for periods longer than 1 h led to the gradual proteolytic loss of the C-terminal AE2 epitope. In contrast, trypsinization of detergent-solubilized pig AE2 in the presence of antibody led to rapid accumulation of T20, in a yield almost 2 orders of magnitude higher than the yields of P35 or P28 from the same quantity of membrane protein. Sequencing of T20 revealed two nearby cleavage sites hydrolyzed at different rates (Figure 6C). The principal cleavage site corresponded to the intracellular T20 site determined by Jennings et al. 1986) for human AE1. The minor AE2 cleavage site Lys-Ile, which produced the shorter fragment, is not conserved in AE1. The AE1 and AE2 sequences between these two tryptic sites are only 33% identical, whereas that in both adjacent putative transmembrane segments is 85%−90%. Thus, the sequence between the two tryptic sites likely represents the 10−11 endofacial loop of AE2, but direct proof for its intracellular disposition is lacking.

Neither native erythroid AE1 nor its membrane-associated domain purified in the detergent $C_{12}E_8$ displayed altered sensitivity to trypsin or to proteinase K following enzymatic deglycosylation (Casey et al., 1992), but the effects on chymotryptic cleavage were not reported. Deglycosylation with PNGase F of gastric membranes from pig or rabbit similarly left tryptic susceptibility of AE2 unchanged but unmasked new AE2 chymotryptic cleavage sites which differed in the two species. In pig, the unmasked chymotryptic sites were located in the AE2 7−8 ecto-loop, producing C-terminal fragments of 28 and 29 kDa. These cleavages were evident only at low ionic strength, and were not observed at physiological ionic strength. The unmasked sites suggested direct or indirect interaction between AE2 oligosaccharide in the Z-loop with the amino acids of the 7−8 ecto-loop.

Even at low ionic strength, the Z-loop of native rabbit AE2 appeared resistant to chymotryptic cleavage. If cleavage within the Z-loop did occur, it proceeded more slowly than proteolytic removal of the C-terminal epitope which would abolish ability to detect the C-terminal fragment. However, deglycosylation of rabbit AE2 unmasked a new chymotryptic site in the Z-loop, CH35 (Figure 3C). This unmasked site likely resides between Arg879 (T36) and Gly888 (the predicted P35 site in rabbit AE2). Though there are within this region no amino acid residues with bulky neutral side chains which serve as the usual target for chymotryptic attack, serines at positions 880 and 881, as well as glutamines at positions 884 and 887 could fulfill this function (Smyth, 1967). The location of this site near the glycosylated Asn residue(s) of the protein is consistent with simple removal of a steric block to chymotrypsin access. The protective role of N-linked oligosaccharides against in-membrane proteolysis at cleavage sites adjacent to and distant from glycosylated Asn residues(s) had not previously been demonstrated for proteins of the AE gene family. Recently, a binding interaction between oligosaccharide residues and amino acid residues located at a distance from the glycosylation anchor site was documented in the crystal structure of the glycosylated lymphocyte surface costimulatory antigen, CD2 (Wyss et al., 1995).

AE2 of pig gastric membranes displayed heterogeneity of N-linked glycosylation. Though not evident in the diffuse band of the holoprotein, several discrete membrane-associated C-terminal AE2 glycopeptides were detectable following digestion with trypsin (Figure 1) or with chymotrypsin (Figure 3). Subsequent complete N-deglycosylation of these sets of glycopeptide digestion products produced better resolved, single bands which nonetheless remained diffuse, thus confirming that proteolytic degradation did not explain the initial heterogeneity. Heterogeneity of glycosylation has been well documented for the single N-linked oligosaccharide of erythroid AE1 (Fukuda et al., 1984; Tsuji et al., 1981) and is common among glycoproteins (Opdenakker et al., 1993). In pig AE2 the heterogeneity of T55 must arise from variable N-linked glycosylation of Asn 64 (Figure 6A), which corresponds to residue 878 of mouse AE2. Localization of other possible N-linked oligosaccharides in AE2 will require genetic modification of recombinant AE2, or direct chemical analysis of this region of the protein.

The low-resolution AE1 structure obtained from two-dimensional crystals of deglycosylated AE1 (Wang et al., 1993) was interpreted as showing dimers of membrane domains. Each domain consisted of three subdomains, two of which appeared to share a large surface at the dimer interface (Wang et al., 1993). The SDS-resistant dimerization of AE2 C-terminal proteolytic fragments (Figures 1−4) suggests that a similar dimer interface resides within the C-terminal 28 kDa of AE2 (encompassing the seven C-terminal putative TM spans). This SDS-resistant dimerization of AE2 was not observed in immunoblots of membranes solubilized in SDS immediately after preparation, or maintained at 4 °C for brief periods. However, SDS-resistant dimerization appeared to increase as a function of time of incubation of membranes at 37 °C (not shown). This behavior of a protein present in ∼0.1% abundance in gastric mucosal membranes (and up to ≤1% in the basolateral membrane of the parietal cell) suggests that AE2 could exist as a dimer in the native membrane.

The proteolytic analysis of native and partially denatured AE2 presented in the current work will serve as a useful point of comparison for evaluation of future topographical studies to be performed with recombinant wild-type and mutant AE2s. In addition, these studies suggest that interactions between oligosaccharides and adjacent polypeptide chains are of biochemical consequence and may have physiological importance, as well.

ACKNOWLEDGMENT

We thank Ms. Tatiana Zolotarev for technical assistance, Dr. Richard Cook for amino acid sequencing, and Dr. Robert Johnson for access to pig tissue. Drakoulis Yannoukakos was a postdoctoral fellow of the Massachusetts Affiliate of the American Heart Association. Seth L. Alper is an Established Investigator of the American Heart Association.

REFERENCES

Alper, S. L., Kopito, R. R., Libresco, S. M., & Lodish, H. F. (1988) *J. Biol. Chem. 263,* 17092−17099.

Alper, S. L., Natale, J., Gluck, S., Lodish, H. F., & Brown, D. (1989) *Proc. Natl. Acad. Sci. U.S.A. 86*, 5429−5433.
Arnon, R. (1970) *Methods Enzymol. 19*, 226−244.
Casey, J. R., Pirraglia, C. A., & Reithmeier, R. A. F. (1992) *J. Biol. Chem. 267*, 11940−11948.
Chirgwin, J. M., Przybyla, A. E., McDonald, R. J., & Rutter, W. J. (1979) *Biochemistry 18*, 5294−5299.
Chow, A., Dobbins, J. W., Aronson, P. S., & Igarashi, P. (1992) *Am. J. Physiol. 263 (Gastrointest. Liver Physiol. 26)*, G345-G352.
Fukuda, M., Dell, A., Oates, J. E., & Fukuda, M. N. (1984) *J. Biol. Chem. 259*, 8260−8273.
Gehrig, H., Muller, W., & Appelhans, H. (1992) *Biochim. Biophys. Acta 1130*, 326−328.
Harlow, E., & Lane, D. (1988) *Antibodies: A Laboratory Manual*, p 123, Cold Spring Harbor Laboratory Press, New York.
He, X., Wu, X., Knauf, P. A., Tabak, L. A., & Melvin, J. E. (1993) *Am. J. Physiol. 264 (Cell Physiol. 33)*, C1075-C1079.
Hennessey, J. P., & Scarborough, G. A. (1989) *Anal. Biochem. 176*, 284−289.
Humphreys, B. D., Jiang, L., Chernova, M. N., & Alper, S. L. (1994) *Am. J. Physiol. 266 (Cell Physiol. 36)*, C1295-C1307.
Jenkins, R. E., & Tanner, M. J. A. (1977) *Biochem. J. 161*, 131−138.
Jennings, M. L. (1992) in *The Kidney:Physiology and Pathophysiology* (Seldin, D. W., & Giebisch,G., Eds.) pp 503−535, Raven Press, New York.
Jennings, M. L., Adams-Lackey, M., & Denney, G. H. (1984) *J. Biol. Chem. 259*, 4652−4660.
Jennings, M. L., Anderson, M. P., & Monaghan, R. (1986) *J. Biol. Chem. 261*, 9002−9010.
Jiang, L., & Alper, S. L. (1993) *J. Am. Soc. Nephrol. 4*, 841a.
Kawasaki, E. S. (1990) in *PCR Protocols: A Guide to Methods and Applications* (Innis, M. A., Gelfand, D. H., Sninsky, J. J., & White, T. J., Eds.) pp 21−27, Academic Press, New York.
Kohler, G., & Milstein, C. (1976) *Eur. J. Immunol. 6*, 511−519.
Laemmli, U. K. (1970) *Nature (London) 227*, 680−685.
Landolt-Marticorena, C., Casey, J. R., & Reithmeier, R. A. F. (1995) *Mol. Membr. Biol. 12*, 173−182.
Lee, B. S., Gunn, R. B., & Kopito, R. R. (1991) *J. Biol. Chem. 266*, 11448−11454.
LeGendre, N., & Matsudaira, P. (1989) in *A Practical Guide to Protein and Peptide Purification for Microsequencing* (Matsudaira, P. T., Ed.) pp 49−69, Academic Press, Inc., New York.
Lindsey, A. E., Schneider, K., Simmons, D. M., Baron, R., Lee, B. S., & Kopito, R. R. (1990) *Proc. Natl. Acad. Sci. U.S.A. 87*, 5278−5282.
Makino, S., Moriyama, R., Kitahara, T., & Koga, S. (1984) *J. Biochem. 95*, 1019−1029.
Mawby, W. J., & Findlay, J. B. C. (1982) *Biochem. J. 205*, 465−475.
Okubo, K., Kang, D., Hamasaki, N., & Jennings, M. L. (1994) *J. Biol. Chem. 269*, 1918−1926.
Opdenakker, G., Rudd, P. M., Ponting, C. P., & Dwek, R. A. (1993) *FASEB J. 7*, 1330−1337.
Raida, M., Wendel, J., Kojro, E., Fahrenholz, F., Fasold, H., Legrum, B., & Passow, H. (1989) *Biochim. Biophys. Acta 980*, 291−298.
Ran, S., & Benos, D. J. (1992) *J. Biol. Chem, 267*, 3618−3625.
Smyth, D. G. (1967) *Methods Enzymol. 11*, 214−231.
Stuart-Tilley, A., Sardet, C., Pouyssegur, J., Schwartz, M. A., Brown, D., & Alper, S. L. (1994) *Am. J. Physiol. 266 (Cell Physiol. 35)*, C559-C568.
Sweadner, K. J. (1991) *Anal. Biochem. 194*, 130−135.
Tarentino, A. L., Quinones, G., Tramble, A., Changchien, L.-M., Duceman, B., Maley, F., & Plummer, T. H. (1990) *J. Biol. Chem. 265*, 6961−6966.
Tsuji, T., Irimura, T., & Osawa, T. (1981) *J. Biol. Chem. 256*, 10497−10502.
Wang, D. N., Kuhlbrandt, W., Sarabia, V. E., & Reithmeier, R. A. F. (1993) *EMBO J. 12*, 2233−2239.
Wang, D. N, Sarabia, V. E., Reithmeier, R. A. F., & Kuhlbrandt, W. (1994) *EMBO J. 13*, 3230−3235.
Wood, P. G. (1992) *Prog. Cell Res. 2*, 325−352.
Wyss, D. F., Choi, J. S., Li, J., Knoppers, M. H., Willis, K. J., Arulanandam, A. R. N., Smolyar, A., Reinherz, E. L., & Wagner, G. (1995) *Science 269*, 1189−1312.
Yannoukakos, D., Stuart-Tilley, A., Fernandez, H. A., Fey, P., Duyk, G., & Alper, S. L. (1994) *Circ. Res. 75*, 603−614.
Zhang, Y., Chernova, M., Stuart-Tilley, A., Jiang, L., & Alper, S. L. (1996) *J. Biol. Chem. 271*, 5741−5749.
Zolotarev, A. S., & Alper, S. L. (1993a) *J. Am. Soc. Nephrol. 4*, 851a.
Zolotarev, A. S., & Alper, S. L. (1993b) *Gastroenterology 104* (Suppl. 4), A232.
Zolotarev, A. S., Townsend, R. R., Stuart-Tilley, A., & Alper, S. L. (1996) *Am. J. Physiol. (Gastrointest. Liver Physiol.)* (in press).

BI9526084